

End-to-End Multi-Core Fibre Transmission Link Enabled by Silicon Photonics Transceiver with Grating Coupler Array

Tetsuya Hayashi⁽¹⁾, Attila Mekis⁽²⁾, Tetsuya Nakanishi⁽¹⁾, Mark Peterson⁽²⁾, Subal Sahn⁽²⁾, Peng Sun⁽²⁾, Steven Freyling⁽²⁾, Gene Armijo⁽²⁾, Chang Sohn⁽²⁾, Dennis Foltz⁽²⁾, Thierry Pinguet⁽²⁾, Michael Mack⁽²⁾, Yasuomi Kaneuchi⁽¹⁾, Osamu Shimakawa⁽¹⁾, Tetsu Morishima⁽¹⁾, Takashi Sasaki⁽³⁾, and Peter De Dobbelaere⁽²⁾

⁽¹⁾ Optical Communications Laboratory, Sumitomo Electric Industries, Ltd., Yokohama, Kanagawa, 244-8588 Japan. t-hayashi@sei.co.jp

⁽²⁾ Luxtera Inc., Carlsbad, CA 92011, USA.

⁽³⁾ Innovation Core SEI, Inc., San Jose, CA 95131, USA.

Abstract We present an end-to-end multi-core fibre transmission link where the 8-core fibre and the corresponding 200 Gb/s silicon photonics transceiver chip were co-designed. We demonstrate equivalent performance between the MCF and a parallel SMF transmission links.

Introduction

Today, high bandwidth (BW) optical interconnects play an important role in improving the performance of large-scale data centres by reducing the bottleneck in the switch I/O BW and the front panel BW¹. The optical channel density can be improved by replacing pluggable modules with on-board optics, and ASIC integrated optics are being intensively studied. At the same time, the space-division multiplexing (SDM) over the multi-core fibre (MCF) has been intensively studied for high-density/-capacity transmission^{2,3}. The use of MCF could improve the BW density of both pluggable modules and ASIC I/O interfaces. To fully leverage the density improvement by the MCF, a fully-integrated end-to-end MCF transmission link without fan-in/fan-out (FIFO) is preferred. For multi-mode MCF (MM-MCF), an end-to-end MCF transmission link has been demonstrated with VCSEL and PD arrays⁴. However, MM-MCF whose every core complies a tight-tolerance high-grade specification—such as OM4 or OM5 for suppressing modal dispersion—would result in a low yield and high cost of the fibre, and thus its practical realization is very challenging. On the other hand, a single-mode MCF (SM-MCF) may have a looser tolerance on each core as with the case of the conventional SMF that inherently has low modal dispersion. SM-MCFs are also compatible with silicon photonics (SiPh) grating couplers (GCs)^{5,6}. However, fully-functional SiPh transceivers (TRxs) with native SM-MCF support without requiring any fan-in/-out or core pitch conversion device have not been reported yet⁵⁻⁷.

In this study, we present an end-to-end MCF transmission link for short-reach applications. SiPh TRx and MCF were cooperatively developed. The MCF TRx is based on a conventional PSM-4 TRx for eight SMFs. The only difference is the GC design and layout for

MCF coupling. We observed no significant penalty due to the MCF transmission link.

MCF transmission link

An eight-core fibre with the 2x4 core layout (2x4-MCF) was designed and fabricated for the developed SiPh TRx, as shown in Fig. 1. We employed the trench-assisted index profile that is the same as what is used in the 125- μm -cladding eight-core fibre for O-band². The cladding diameter of the 2x4-MCF was designed to be 180 μm to support the operating λ of 1490 nm, so that the coating-leakage loss was $<0.001\text{dB/km}$ at 1490 nm and $<0.01\text{dB/km}$ at 1550 nm in design. The measured optical properties and transmission spectra of the 2x4-MCF are shown in Tab. 1 and Fig. 2, respectively. The transmission loss, the total crosstalk (XT) from

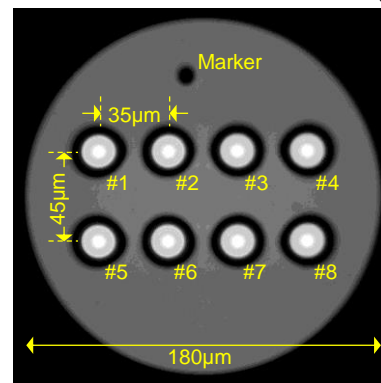


Fig. 1: Cross section of the fabricated 2x4-MCF.

Tab. 1: Optical properties of the fabricated 2x4-MCF

Meas. λ [nm] ¹	1310	1490	1550	1625
MFD [μm]	8.4 \pm 0.1	9.2 ²	9.4 \pm 0.1	n/a
Transmission loss [dB/km]	0.340 to 0.380	0.238 to 0.314	0.220 to 0.303	0.244 to 0.351
Total XT [dB] at 1 km	≤ -66 ²	≤ -48 ²	≤ -42	≤ -33
Bend loss [dB/turn]	R=10mm	< 0.01 ³	≤ 0.03	≤ 0.05
	R=5mm	≤ 0.02	≤ 0.08	≤ 0.13
	R=3mm	≤ 0.04	≤ 0.18	≤ 0.28
λ_{cc} [nm]	1190 to 1202			

¹: Except for λ_{cc} . ²: Inter/extrapolation. ³: Lower than the error floor.

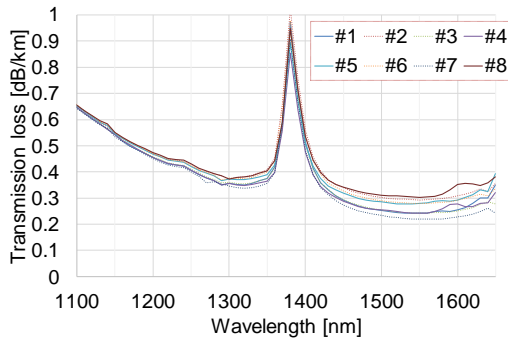


Fig. 2: Transmission loss spectra of the fabricated 2x4-MCF. (Dotted lines: inner cores, solid lines: outer cores)

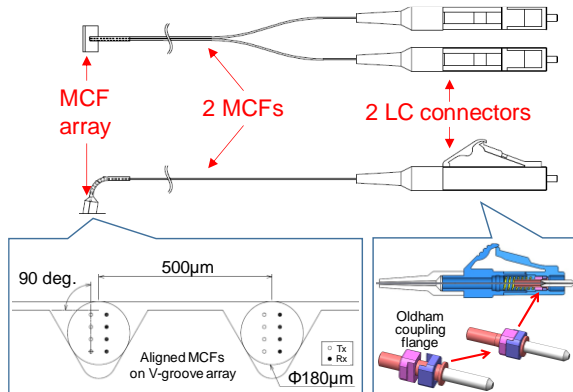


Fig. 3: Schematic of MCF attachment for SiPh TRx.

the neighboring cores, and the bend loss, at 1490 nm, were low enough for short-reach applications. The coating-leakage loss was negligible up to ~1550 nm. The loss variation among the cores gets larger as the wavelength gets longer. We consider that this loss variation was caused by the prototype fabrication process because of its wavelength dependence and because there is no correlation between the loss and core position. Thus we consider the loss can be improved and comparable to the SSMF by refining the process.

Using the 2x4-MCF, we fabricated MCF attachments for SiPh TRx, which are two 2x4-MCFs terminated by one V-groove fiber array and two LC connectors, as shown in Fig. 3. The core position error in the MCF arrays was $0.32 \mu\text{m}$ in the standard deviation of five samples. The LC connectors employed the Oldham coupling⁸ for simultaneously realizing the ferrule floating mechanism and the rotational alignment. The fiber rotational error between two mated LC connectors was $< \pm 1$ degree, which corresponds to $< \pm 1 \mu\text{m}$ core position misalignment.

Silicon Photonics Transceiver Design Natively Supporting MCF

The 200-Gb/s SiPh transceiver module contains eight transmitter (Tx) and receiver (Rx) channels integrated in a single chipset. The chipset comprises a photonic chip, and electronic chip, and a micropackaged light source. The optical modulator and receiver is on the photonic die.

The electronic die contains the analog and digital electronics: the modulator driver, the receiver amplifiers, and the chipset control circuitry.

Two versions of the photonic die with different fibre interfaces were designed, contrasted in Fig. 4. The standard optical interface comprises 8 Tx and 8 Rx GCs arranged in a row at $250 \mu\text{m}$ spacing, matching a standard 16-channel SMF array. There are 8 single-polarization GCs (SPGCs) in the Tx array and 8 polarization-splitting GCs (PSGCs) in the Rx array.

The optical interface of the MCF transceiver chip is significantly more compact. The 8 GCs of each group of four channels are clustered in a configuration to match the MCF cores. The two sets of eight GCs are separated from each other by $500 \mu\text{m}$. The MCF die optical interface attains a very high throughput density ($> 100 \text{ Tb/s/mm}^2$).

One challenge posed by the compact MCF is enabling the 12 waveguide escapes from the tightly packed 2x4 GC array (Fig. 5). To achieve this, the Tx SPGC was designed such that its waveguide encloses a 45° angle with the fiber tilt plane. On the Rx side, the two outputs of the Rx PSGCs are connected to the same on-chip photodetector, and so each channel creates a closed loop on the chip. For this reason, the four Rx channels were successively enclosed within each other to avoid waveguide crossings.

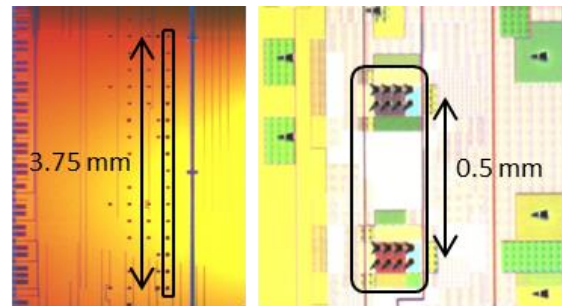


Fig. 4: Optical micrograph of the SMF (left) and the MCF (right) chip optical interfaces.

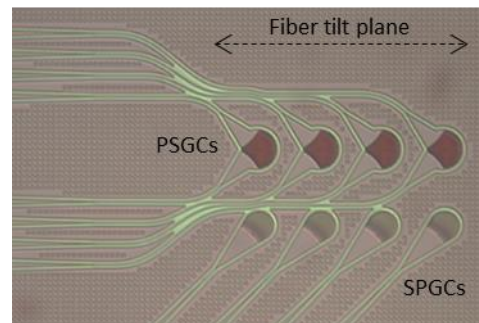


Fig. 5: Close-up view of the MCF chip interface.

Experimental results

To assess the performance of the MCF-GC interface, the total insertion loss (IL) of the Tx-to-Rx external loopback was measured for all channels and compared to the SMF TRxs. This

loss number includes the fiber-GC coupling loss on the Tx and Rx sides, along with any penalties added by the external connectors and the fiber-array attach process during module assembly. The IL of some of the photonic elements in the path (detector responsivity penalty, waveguide loss, monitoring tap losses) has not been de-embedded since they are common to both types of modules. The results of the comparison are shown in Fig. 6. The data is for 2 MCF modules and 3 SMF modules. The MCF parts show an average of 0.8 dB excess loss, but this is within the overall variability expected in such a measurement over such a small sample size. It can be concluded that the MCF arrays result in performance comparable to our baseline 8x transceivers.

The impact of going to the edge of the short-reach window with MCF was assessed by connecting two transceivers through 500m long

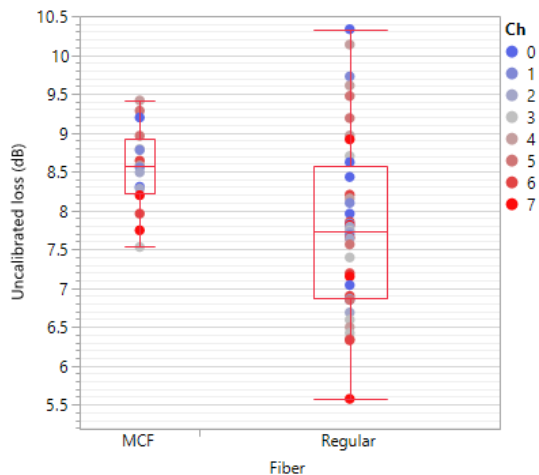


Fig. 6: Loss in an external loopback test for 8 lane transceivers built with MCF and SMF.

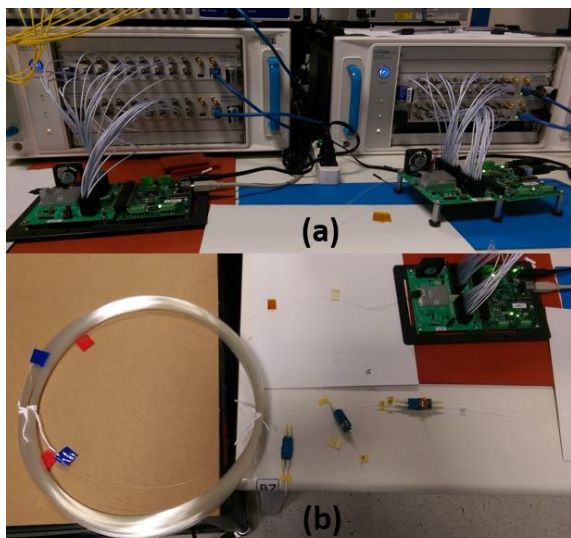


Fig. 7: Setup testing 2 MCF 200-Gbps transceivers. (a) 2 modules in evaluation boards connected to BERTs. (b) 500 m MCF spools that connect the two modules, creating two bidirectional 4x25 Gbps links.

spools of MCF (Fig. 7). Each spool establishes bidirectional 4x25-Gb/s links between the two modules. The insertion loss of the 500 m long fibers was assessed through the change in Rx photocurrents when they were introduced in the link, and it was found to be 0.2 dB on average. Bathtub BER measurements followed with and without the 500 m spools in the link. The results in Fig. 8 show that the additional MCF length adds no dynamic penalty to the link performance.

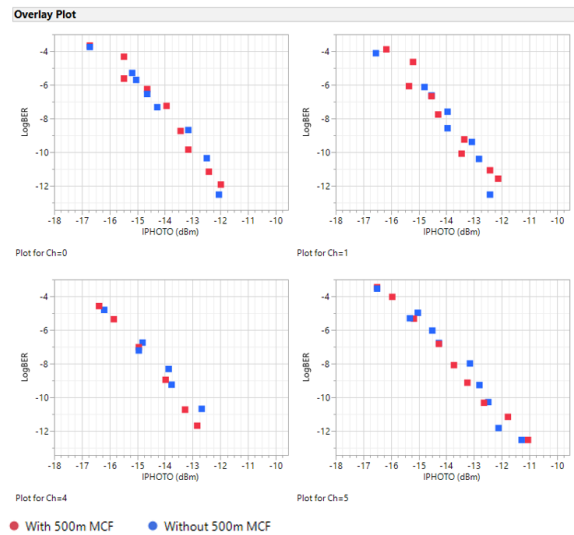


Fig. 8: BER bathtub curves with and without 500m MCF spools in the link. Two lanes from each of the two 4x25Gbps bidirectional links are shown.

Conclusions

We co-designed the eight-core fibre and the corresponding SiPh transceiver chip, and realized the end-to-end MCF transmission link with fully-functional bidirectional 200-Gb/s (2 MCFs x 4 cores x 25 Gb/s) SiPh transceivers, without any significant BER penalty due to the MCF. The results demonstrated the high compatibility of the SiPh and the MCF, and the potential of the MCF transmission link terminated with the corresponding native SiPh transceivers for short-reach applications.

References

- [1] A. Ghiasi, *Opt. Express*, Vol. **23**, no. 3, pp. 2085–2090 (2015).
- [2] T. Hayashi et al., *J. Lightw. Technol.*, Vol. **34**, no. 1, pp. 85–92 (2016).
- [3] T. Morishima et al., in *OFC, Th5D.4*, Los Angeles (2017).
- [4] B. G. Lee et al., *J. Lightw. Technol.*, Vol. **30**, no. 6, pp. 886–892 (2012).
- [5] T. Pinguet et al., in *IEEE Photon. Soc. Sum. Top., WC4.1*, Seattle (2012).
- [6] Y. Ding et al., *Opt. Express*, Vol. **23**, no. 3, pp. 3292–3298 (2015).
- [7] P. D. Heyn et al., in *OFC, Th1B.7*, Los Angeles (2017).
- [8] R. Nagase et al., *IEICE Trans. Electron.*, Vol. **E96-C**, no. 9, pp. 1173–1177 (2013).